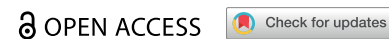


RESEARCH ARTICLE



Design, synthesis, and biological evaluation of (thio)urea derivatives as potent *Escherichia coli* β -glucuronidase inhibitors

Keren Xu^a, Leyi Ying^a, Titi Ying^a, Qihao Wu^{a,b}, Lin Du^c, Yanlei Yu^a, Youmin Ying^a, Bin Wei^{a,d}, Hong Wang^a and Zhikun Yang^{a,d}

^aCollege of Pharmaceutical Science & Green Pharmaceutical Collaborative Innovation Center of Yangtze River Delta Region, Key Laboratory of Marine Fishery Resources Exploitation & Utilization of Zhejiang Province, Zhejiang University of Technology, Hangzhou, China; ^bDepartment of Chemistry, Institute of Biomolecular Design & Discovery, Yale University, West Haven, CT, USA; ^cMinistry of Education & College of Agronomy and Biotechnology, China Agricultural University, Beijing, China; ^dBinjiang Cyberspace Security Institute of Zhejiang University of Technology, Hangzhou, China

ABSTRACT

EcGUS has drawn considerable attention for its role as a target in alleviating serious GIAEs. In this study, a series of 72 (thio)urea derivatives were designed, synthesised, and biologically assayed. The bioassay results revealed that **E-9** ($IC_{50} = 2.68 \mu M$) exhibited a promising inhibitory effect on EcGUS, surpassing EcGUS inhibitor D-saccharic acid-1,4-lactone (DSL, $IC_{50} = 45.8 \mu M$). Additionally, the inhibitory kinetic study indicated that **E-9** ($K_i = 1.64 \mu M$) acted as an uncompetitive inhibitor against EcGUS. The structure-activity relationship revealed that introducing an electron-withdrawing group into the benzene ring at the *para*-position is beneficial for enhancing inhibitory activity against EcGUS. Furthermore, molecular docking analysis indicated that **E-9** has a strong affinity to EcGUS by forming interactions with residues Asp 163, Tyr 472, and Glu 504. Overall, these results suggested that **E-9** could be a potent EcGUS inhibitor, providing valuable insights and guidelines for the development of future inhibitors targeting EcGUS.

ARTICLE HISTORY

Received 10 June 2024
Revised 13 July 2024
Accepted 18 July 2024

KEYWORDS



β -Glucuronidase inhibitor;
(thio)urea derivatives;
structure-activity
relationship; gastrointestinal
adverse events


Introduction

Gastrointestinal adverse events (GIAEs) are common occurrences in daily life, presenting symptoms that ranging from nausea and fever to dehydration, with severe cases frequently leading to colitis, hepatitis, or pancreatitis^{1,2}. The overexpression of the acidic hydrolase β -glucuronidase (β GLUS) in cytolysosomes contributes to the pathogenesis of GIAEs by catalysing the hydrolysis of glucuronides associated with medicines, hormones, and proteoglycans³. Consequently, the accumulation of aglycones resulting from glucuronide deglycosylation inside the intestine poses a significant health risk due to their potent toxicity, implicated not only in matrix degradation during tumour invasion and metastasis, but also in influencing various pharmacokinetic behaviours⁴⁻⁸. Irinotecan (CPT-11) is commonly used as a chemotherapeutic agent for colorectal cancer (CRC). Nevertheless, it is associated with undeniable adverse effects due to the hydrolysis of its inactive glucuronic acid metabolite by β GLUS, which generates 7-ethyl-10-hydroxycamptothecin (SN-38). This process results in GIAEs characterised by mucosal damage⁹. Additionally, carboxylic acid-containing non-steroidal anti-inflammatory drugs (NSAIDs), especially Indomethacin and Diclofenac, are hindered in their usage due to the risk of inducing intestinal damage facilitated by enterohepatic circulation. Studies indicate that a substantial proportion of both long-term (>3 months) and short-term (>1 week)

users experience varying degrees of intestinal injury¹⁰⁻¹². Therefore, it is essential to investigate interventions that directly inhibit β GLUS to reduce intestinal toxicity during drug metabolism.

For *Escherichia coli* β -glucuronidase (EcGUS), its asymmetric unit contains two monomers of 597 ordered residues. The *N*-terminal 180 residues resemble the sugar-binding domain of family 2 glycosyl hydrolases, whereas the *C*-terminal domain (residues 274 to 603) forms an $\alpha\beta$ barrel and contains the active-site residues Glu 413 and Glu 504. The region between the *N*- and *C*-terminal domains exhibits an immunoglobulin-like β -sandwich domain. The loop (residues 360 to 376) forms direct contact with the bound inhibitors in the EcGUS, which is labelled the "bacterial loop"⁴. Through high-throughput screening (HTS), several Food and Drug Administration (FDA)-approved drugs, including nialamide, isocarboxazid, phenelzine (monoamine oxidase inhibitors, MAOIs), amoxapine (AMX, a tricyclic antidepressant), and mefloquine (an antimalarial) (Figure 1), were found to exhibit remarkable inhibitory activity against EcGUS¹³. As a representative EcGUS inhibitor with potential, D-saccharic acid-1,4-lactone (DSL, Figure 1) was used to protect intestinal mucosa from CPT-11-induced diarrhoea or injury and to inhibit tumour growth in mice without selectivity¹⁴. However, despite its safety profile, the efficacy of DSL is limited by its poor stability under normal physiological conditions and its inability to adequately inhibit the *p*-nitrophenyl- β -D-glucuronide (PNPG)-hydrolyzing activity of human gut microbiota, particularly in

CONTACT Zhikun Yang  yangzk@zjut.edu.cn  College of Pharmaceutical Science & Green Pharmaceutical Collaborative Innovation Center of Yangtze River Delta Region, Zhejiang University of Technology, Hangzhou, 310014, China.

 Supplemental data for this article can be accessed online at <https://doi.org/10.1080/14756366.2024.2387415>.

© 2024 The Author(s). Published by Informa UK Limited, trading as Taylor & Francis Group
This is an Open Access article distributed under the terms of the Creative Commons Attribution-NonCommercial License (<http://creativecommons.org/licenses/by-nc/4.0/>), which permits unrestricted non-commercial use, distribution, and reproduction in any medium, provided the original work is properly cited. The terms on which this article has been published allow the posting of the Accepted Manuscript in a repository by the author(s) or with their consent.

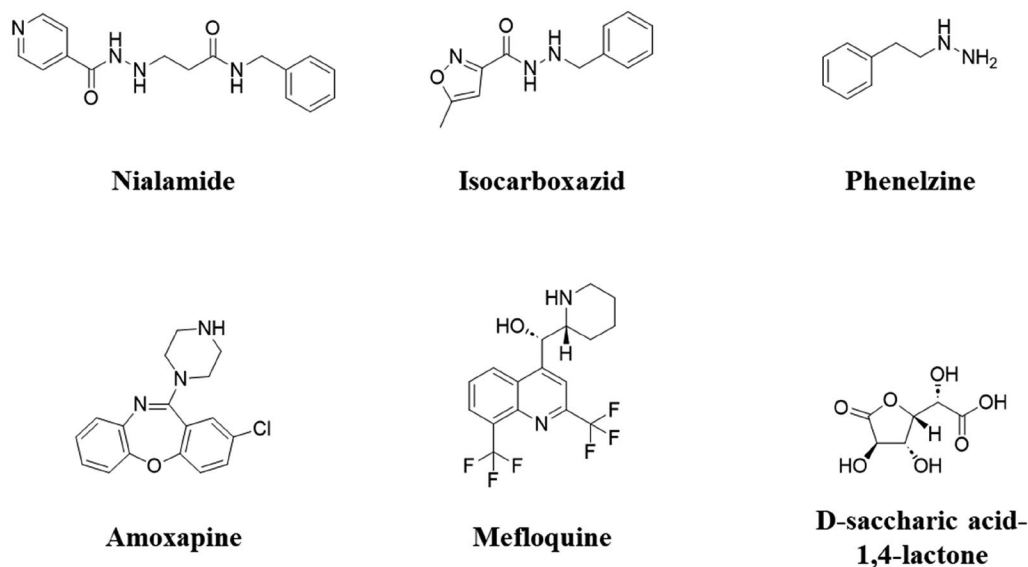


Figure 1. Chemical structures of emblematic drugs against side effects of CPT-11.

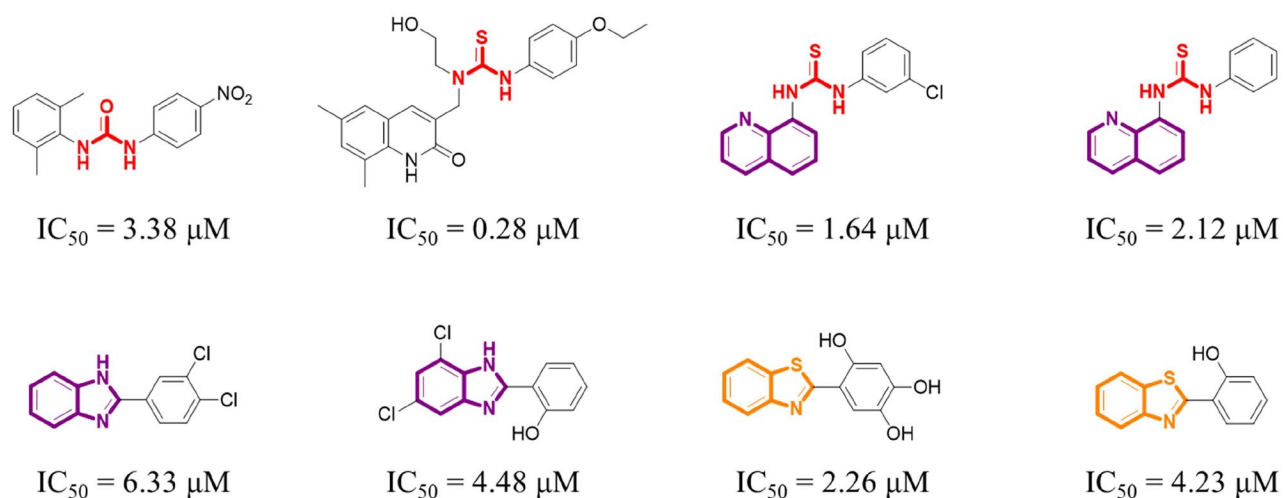


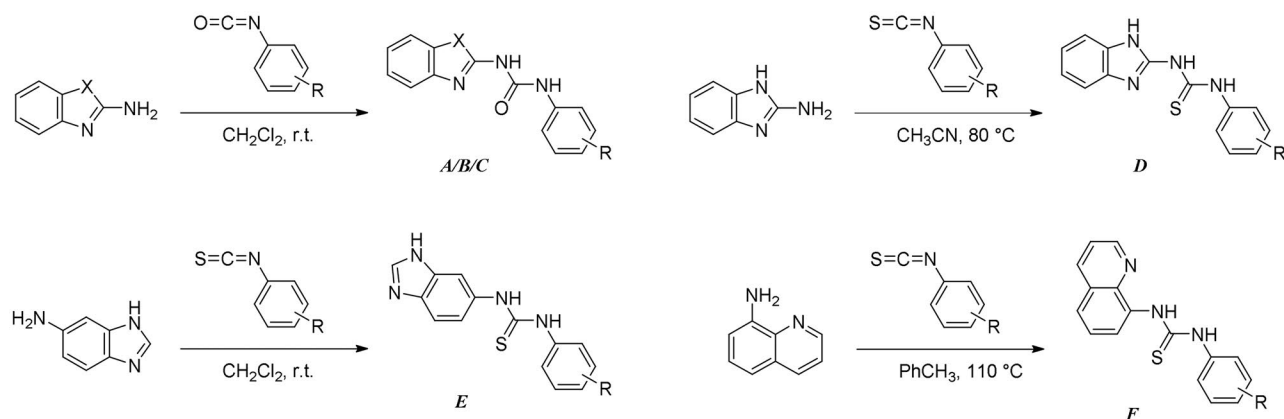
Figure 2. Chemical structures of representative EcGUS inhibitors.

advanced therapeutic stages^{15,16}. These limitations underscore the necessity for continued research aimed at discovering novel lead compounds with potent inhibitory activity against EcGUS.

In recent years, different types of naturally occurring EcGUS inhibitors, including flavonoids, terpenoids, steroids, iminosugars, and other plant extracts, have been discovered^{17–25}. However, in most cases, due to limited access to natural sources, purifying active natural products is challenging and can only provide limited materials for subsequent investigations. Considering this, chemical synthesis could offer advantages in obtaining lead compounds with streamlined processes and sufficient yields. Therefore, there is a need for chemically synthesised inhibitors to advance more treatment options aim at maintaining intestinal health^{26–28}.

Previously, it was found that 1-(6,8-dimethyl-2-oxo-1,2-dihydroquinolin-3-yl)-3-(4-ethoxyphenyl)-1-(2-hydroxyethyl)thiourea (**Figure 2**) exhibited significant inhibitory activity against EcGUS, thereby alleviating intestinal injury caused by NSAIDs²⁹. Importantly,

(thio)urea skeleton, which readily forms intermolecular hydrogen bonds with various biological enzymes, has been widely utilised in diverse therapeutic fields with extensive applications^{30,31}. Additionally, other small molecules (**Figure 2**) containing benzoheterocyclic rings, such as benzimidazole, benzothiazole, or quinoline, have also shown evident biological activity against EcGUS^{32–43}. In this study, we aimed to further explore potential synthetic inhibitors of EcGUS. To achieve this, we designed and synthesised six sets of skeletons comprising 72 (thio)urea derivatives. Subsequently, their *in-vitro* activities were investigated, and the resulting structure-activity relationship (SAR) was thoroughly discussed. Additionally, their pharmacokinetic properties were preliminarily assessed by predicting their respective oil-water distribution coefficients (**Log P**). Following that, an inhibition kinetics study of the optimal compound **E-9** was performed to further investigate its functional mechanism, and molecular docking was conducted to analyse its binding properties with the EcGUS receptor.



Scheme 1. Synthetic routes of target compounds.

Materials and methods

Chemicals and instruments

All reactants and solvents were purchased from Bidepharm (Shanghai, China) and Tansooe (Shanghai, China). All commercially available reagents were of analytical grade (purity >98%) and simply used without further purification. The reaction progress was monitored by thin-layer chromatography (TLC) on silica gel GF-254 and detected under ultraviolet light (UV, 254 nm). Column chromatography was carried out using silica gel (200–300 mesh). Specially, the substrate was provided by Yuanye Bio-Technology (Shanghai, China), and the enzyme was provided by Merck (Shanghai, China), the positive control inhibitors were supplied by MedChemExpress (Shanghai, China). The spectra of ^1H NMR and ^{13}C NMR were obtained at 500 and 125 MHz, respectively, using a Bruker AVANCE DPX500 spectrometer in $\text{DMSO}-d_6$ solution with tetramethylsilane (TMS) as the internal standard. HRMS were performed using an AB X500B Q-TOF LC/MS system, equipped with an electrospray ionisation (ESI) source in the positive ionisation mode. The data of absorbance under 405 nm ($\text{OD}_{405\text{nm}}$) were obtained using a SpectraMax-iD3 Multi-Mode Microplate Reader (MOLECULAR DEVICES, America).

General synthesis

The synthetic routes of target compounds **A-1** to **11**, **B-1** to **11**, **C-1** to **11**, and **D-1** to **13**, **E-1** to **13**, and **F-1** to **13** were outlined in Scheme 1. Among these synthetic compounds, the novel ones include **B-1**, **B-2**, **B-3**, **B-5**, **B-7**, **B-8**, **B-9**, **B-10**, **B-11**; **D-1**, **D-2**, **D-7**, **D-10**, and **D-12**.

General preparative procedure for 1-(1*H*-benzo[*d*]imidazol-2-yl)-3-(2-fluorophenyl)urea (**A-1**). 2-Fluorophenyl isocyanate (0.061 ml, 0.5 mmol, 1.0 eqv.) was added dropwise to a solution of equivalent 2-amino benzimidazole (0.067 g, 0.5 mmol, 1.0 eqv.) in dichloromethane (5 ml). Then, the reaction mixture was stirred at room temperature for 2 h. After complete reaction, the solvent was evaporated by vacuum, and a white solid was obtained (96%, yield), named **A-1**. Other compounds (**A-2** to **11**) were synthesised using the same methodology above.

General preparative procedure for 1-(benzo[*d*]oxazol-2-yl)-3-(2-fluorophenyl)urea (**B-1**). 2-Fluorophenyl isocyanate (0.061 ml, 0.5 mmol, 1.0 eqv.) was added dropwise to a solution of equivalent 2-amino benzoxazole (0.067 g, 0.5 mmol, 1.0 eqv.) in dichloromethane (5 ml). Then, the reaction mixture was stirred at room

temperature for 2 h. After complete reaction, the solvent was evaporated by vacuum, and a yellow solid was obtained (96%, yield), named **B-1**. Other compounds (**B-2** to **11**) were synthesised using the same methodology above.

General preparative procedure for 1-(benzo[*d*]thiazol-2-yl)-3-(2-fluorophenyl)urea (**C-1**). 2-Fluorophenyl isocyanate (0.061 ml, 0.5 mmol, 1.0 eqv.) was added dropwise to a solution of equivalent 2-amino benzothiazole (0.075 g, 0.5 mmol, 1.0 eqv.) in dichloromethane (5 ml). Then, the reaction mixture was stirred at room temperature for 2 h. After complete reaction, the solvent was evaporated by vacuum, and a white solid was obtained (96%, yield), named **C-1**. Other compounds (**C-2** to **11**) were synthesised using the same methodology above.

General preparative procedure for 1-(1*H*-benzo[*d*]imidazol-2-yl)-3-(2-fluorophenyl)thiourea (**D-1**). 2-Fluorophenyl isothiocyanate (0.067 ml, 0.5 mmol, 1.0 eqv.) was added to a solution of equivalent 2-amino benzimidazole (0.067 g, 0.5 mmol, 1.0 eqv.) in anhydrous acetonitrile (5 ml) under argon atmosphere. Then, the reaction mixture was refluxed at 80 °C for 4 h, and then allowed to cool down to room temperature. After complete reaction, the solvent was evaporated by vacuum, and a beige solid was obtained (93%, yield), named **D-1**. Other compounds (**D-2** to **13**) were synthesised using the same methodology above.

General preparative procedure for 1-(1*H*-benzo[*d*]imidazol-6-yl)-3-(2-fluorophenyl)thiourea (**E-1**). 2-Fluorophenyl isothiocyanate (0.067 ml, 0.5 mmol, 1.0 eqv.) was added to a solution of equivalent 6-amino benzimidazole (0.067 g, 0.5 mmol, 1.0 eqv.) in dichloromethane (5 ml). Then, the reaction mixture was stirred at room temperature for 2 h. After complete reaction, the solvent was evaporated by vacuum, and a white solid was obtained (98%, yield), named **E-1**. Other compounds (**E-2** to **13**) were synthesised using the same methodology above.

General preparative procedure for 1-(quinolin-8-yl)-3-(2-fluorophenyl)thiourea (**F-1**). 2-Fluorophenyl isothiocyanate (0.067 ml, 0.5 mmol, 1.0 eqv.) was added to a solution of equivalent 8-aminoquinoline (0.072 g, 0.5 mmol, 1.0 eqv.) in toluene (5 ml) under argon atmosphere. Then, the reaction mixture was refluxed at 110 °C for 5 h, and then allowed to cool down to room temperature. After complete reaction, the solvent was evaporated by vacuum, and a tan solid was obtained (92%, yield), named **F-1**. Other compounds in this class (**F-2** to **13**) were synthesised using the same methodology above.

The detailed characterisation data of ^1H NMR, ^{13}C NMR, and HRMS as well as the ^1H NMR and ^{13}C NMR spectra images are shown in [Supplementary Materials](#).

Biological assay

Synthesised (thio)urea derivatives were subjected to screening for potent inhibitors, and their inhibitory effects were determined by measuring the formation of *p*-nitrophenol (PNP) generated from PNPG by EcGUS in the presence of phosphate-buffered saline (PBS). Solutions of AMX and DSL (10 mM) were prepared in DMSO and stored at 4 °C. The biological activities of test compounds were assayed in accordance with the following detailed procedures:

Briefly, the assays were performed in 96-well flat-bottomed tissue culture plates (Nunc, Denmark) and every well with a total volume of 100 µL, including 10 µL EcGUS (final concentration = 2.0 µg/mL), 70 µL PBS (pH 7.4), 10 µL AMX/DSL, DMSO, or test compound, and 10 µL PNPG (2.5 mM). The order of adding reagents is as follows: enzyme, buffer solution, inhibitor, and substrate. All reactions were performed in triplicate, and the activity of EcGUS was measured by detecting $\Delta OD_{405\text{nm}}$ in a plate reader before/after incubation at 37 °C for 30 min. By setting a standard curve (0, 10, 20, 40, 60, and 80 µM) in PBS, the concentration of PNP was further determined. The relative activities of experimental groups were calculated by comparing the concentration of generated PNP with that of blank control group.

When preparing the corresponding solution for primary screening, the concentration of positive control inhibitor was prescribed as 1 mM (final concentration = 100 µM). After that, partial compounds (inhibitory rate >50%) were chosen for secondary screening, the concentration was set to 0.1 mM (final concentration = 10 µM). The inhibitory rates of EcGUS were calculated according to the following equations:

$$x = \Delta OD_{405\text{nm}} = OD_{30\text{min}} - OD_{0\text{min}}$$

$$y = \Delta C_{\text{PNP}} = c_{30\text{min}} - c_{0\text{min}}$$

$$y = 3.262x \text{ (standard curve)}$$

$$RA = \frac{\Delta C_{\text{EG}}}{\Delta C_{\text{CG}}} \times 100\%$$

$$IR = 1 - RA$$

where x is the difference of $OD_{405\text{nm}}$ values, y is the difference of PNP concentrations, RA is the relative activity of EcGUS in the presence of an inhibitor, respectively, and IR is the corresponding inhibitory rate.

IC_{50} value is defined as the concentration of a sample that required for showing half-maximal inhibition and inhibiting 50% of the activity of EcGUS. K_i value is defined as an inhibitory constant describing the binding ability of inhibitors to enzymes, which is used to measure the ability of drugs to inhibit enzyme activities after binding to target molecules in organisms. To further determine IC_{50} value of test compound *in vitro*, the reaction conditions are as follows: 10 µL EcGUS, 70 µL PBS, 10 µL AMX, DSL, or test compound, and 10 µL PNPG reacting at 37 °C for 30 min. The order of adding reagents is as follows: enzyme, buffer solution, inhibitor, substrate. Besides, the inhibitory behaviour towards EcGUS was also investigated by measuring reaction rates with substrates (2, 3, 5, and 10 mM) and inhibitors in various concentrations. Finally, the type of inhibitor was determined; IC_{50} value and K_i value were calculated.

Molecular docking

For a more in-depth exploration of the molecular interactions between the target compound and EcGUS at the molecular level, molecular docking studies were performed. The target molecular structures of DSL, AMX, and synthetic compounds (**E-9**, **E-4**, **A-9**, **D-9**, and **F-9**) were generated using ChemBioDraw Ultra 13.0 software. Subsequently, these molecular structures were optimised utilising Molecular Operate Environment (MOE) software to prepare them for further molecular docking studies. The receptor EcGUS (PDB code: 3LPF) retrieved from the Protein Data Bank (<https://www.rcsb.org>) was prepared using AutodockTools software. The preparation steps included the removal of water molecules, addition of hydrogen atoms, assignment of Gasteiger charges, and optimisation of nonpolar hydrogen atoms to ensure the receptor was in a suitable conformation for docking studies. The binding pocket of the receptor was identified for the ligand 1-((6,7-dimethyl-2-oxo-1,2-dihydroquinolin-3-yl)methyl)-1-(2-hydroxyethyl)-3-(3-methoxyphenyl)thiourea. This binding pocket involved key residues such as Leu 361, Glu 413, and Asp 163, which are important for ligand-receptor interactions. The definition of the binding pocket was done in the presence of solvent to mimic the physiological conditions where the interactions between the ligand and receptor take place. Utilising the MOE software, molecular docking simulations were executed with meticulous parameterisation, encompassing methodological frameworks such as the triangle matcher for placement and a rigid receptor approach for refinement. The scoring process employed sophisticated algorithms, employing the London dG metric for the initial placement phase and the GBVI/WSA dG method for subsequent refinement. A substantial ensemble of 300 poses was initially generated during the placement stage, with a stringent selection of 5 poses per ligand for refinement. The conformation exhibiting the highest energy favorability among the set of 300 generated poses was meticulously chosen to evaluate the intrinsic potential of the compounds. Following this selection, a comprehensive analysis of the top-tier docking poses was conducted to unravel the intricate molecular interplay between the EcGUS and the target compound.

Statistical analysis

All experiments were carried out in triplicate. All data were representatives of three independent determinations of samples and expressed as mean ± standard deviation (SD). The IC_{50} value was calculated as the necessary concentration of inhibitor that required to bring the curve down to point half way between the top and bottom plateaus. Conveniently, it was evaluated from concentration-response data by nonlinear regression using GraphPad Prism 8.0 (La Jolla, CA). The inhibition type employed a three-parameter curve fit, and it was determined according to the intersection location of Lineweaver-Burk plot: (1) competitive inhibition, intersection at the y-axis; (2) non-competitive inhibition, intersection at the x-axis; (3) uncompetitive inhibition, parallel lines; (4) mixed inhibition, intersection in first or second quadrant.

Results and discussion

Chemical synthesis

Target compounds were prepared through the addition reaction of amine compounds (2-aminobenzimidazole/benzoxazole/benzothiazole, 6-aminobenzimidazole and 8-aminoquinoline), and the key

commercially available intermediates, isocyanates or isothiocyanates. Due to the varying chemical reactivity of the amino groups, the reaction was carried out at different temperatures (room temperature, 80 or 110°C) and in different reaction solvents (dichloromethane, acetonitrile or toluene). Detailed analytical data, including ^1H NMR, ^{13}C NMR, and HRMS of the target compounds, can be found in [supplementary information](#).

Log P prediction of target compounds

As a pharmaceutically critical physicochemical property, **Log P** was calculated by SwissADME⁴⁴. The values of **Log P** of designed compounds fall within an ideal range (2.09–5.44) (Tables 1 and 2), consistent with Lipinski's Rule of Five⁴⁵. Almost all of them conform to the druggability rules in terms of molecular weight (MW) and **Log P** coefficient.

Biological evaluation of test compounds

The inhibitory activity of target (thio)urea derivatives was evaluated and is depicted in Tables 3 and 4, with DSL used as the positive control inhibitor. All compounds were subjected to primary screening at a concentration of 100 μM , wherein a subset of compounds (**C-7**, **C-9**, **E-6**, **E-9**, **E-13**, **F-4**, **F-6**, and **F-13**) exhibited an inhibitory rate exceeding 50%, while the positive control DSL showed an inhibitory rate of 76.2%. These compounds underwent

subsequent evaluation in a secondary screening, employing a reduced concentration of 10 μM . Remarkably, **E-9** showed a better inhibitory activity against EcGUS compared to DSL at 10 μM (Figure 3). **E-9** displayed an inhibitory rate of 72.3%, whereas DSL showed an inhibitory rate of 20.6%, suggesting that **E-9** has superior inhibitory activity against EcGUS. Furthermore, to further elucidate the inhibitory potential, the designed compound **E-9**, along with the positive control inhibitor DSL, were selected for the determination of their IC_{50} values. The results revealed that **E-9** exhibited greater inhibitory effect (IC_{50} = 2.68 μM) compared to DSL (IC_{50} = 45.8 μM). These results demonstrate the potential of **E-9** as a promising candidate for the development of an EcGUS inhibitor.

In the context of SAR, compounds with diverse molecular structures exhibit varied inhibitory effects on EcGUS. As shown in Table 3, the initial screening of urea compounds revealed that with similar substituent groups and positions on the benzene ring, benzothiazole generally exhibits a more significant enhancement in inhibitory activity compared to benzimidazole or benzoxazole analogs. For instance, **C-7** (benzothiazole, R=2- CF_3 , $\text{IR}_{100 \mu\text{M}}$ = 52.9%), **C-8** (benzothiazole, R=3- CF_3 , $\text{IR}_{100 \mu\text{M}}$ = 47.2%), **C-9** (benzothiazole, R=4- CF_3 , $\text{IR}_{100 \mu\text{M}}$ = 58.2%), and **C-10** (benzothiazole, R=3,5-*di*- CF_3 , $\text{IR}_{100 \mu\text{M}}$ = 41.7%) appeared more active than **A-7** (benzimidazole, R=2- CF_3 , $\text{IR}_{100 \mu\text{M}}$ = 27.3%), **A-8** (benzimidazole, R=3- CF_3 , $\text{IR}_{100 \mu\text{M}}$ = 25.3%), **A-9** (benzimidazole, R=4- CF_3 , $\text{IR}_{100 \mu\text{M}}$ = 26.4%), and **A-10** (benzimidazole, R=3,5-*di*- CF_3 , $\text{IR}_{100 \mu\text{M}}$ = 26.8%), as well as **B-7**

Table 1. Predicted **Log P** of target compounds **A** to **C**.

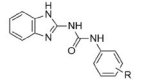
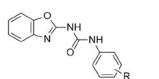
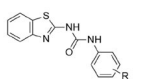
R						
	Compd.	Log P	Compd.	Log P	Compd.	Log P
2-F	A-1	2.43	B-1	2.75	C-1	3.27
3-F	A-2	2.42	B-2	2.69	C-2	3.25
4-F	A-3	2.54	B-3	2.70	C-3	3.25
2-Cl	A-4	2.62	B-4	2.98	C-4	3.51
3-Cl	A-5	2.64	B-5	2.91	C-5	3.47
4-Cl	A-6	2.77	B-6	2.92	C-6	3.48
2- CF_3	A-7	3.19	B-7	3.47	C-7	4.04
3- CF_3	A-8	3.26	B-8	3.49	C-8	4.07
4- CF_3	A-9	3.29	B-9	3.50	C-9	3.89
3,5- <i>di</i> - CF_3	A-10	4.33	B-10	4.55	C-10	5.13
4- OCH_3	A-11	2.09	B-11	2.38	C-11	2.94

Table 2. Predicted **Log P** of target compounds **D** to **F**.

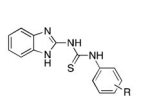
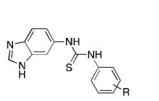
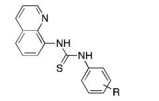
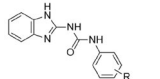
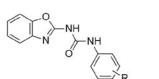
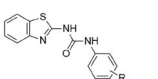
R						
	Compd.	Log P	Compd.	Log P	Compd.	Log P
2-F	D-1	2.94	E-1	2.87	F-1	3.68
3-F	D-2	2.93	E-2	2.92	F-2	3.66
4-F	D-3	2.93	E-3	2.93	F-3	3.66
2-Cl	D-4	3.19	E-4	3.10	F-4	3.89
3-Cl	D-5	3.16	E-5	3.15	F-5	3.86
4-Cl	D-6	3.26	E-6	3.15	F-6	3.88
2- CF_3	D-7	3.69	E-7	3.63	F-7	4.39
3- CF_3	D-8	3.77	E-8	3.59	F-8	4.35
4- CF_3	D-9	3.76	E-9	3.64	F-9	4.37
3,5- <i>di</i> - CF_3	D-10	4.82	E-10	4.68	F-10	5.44
2- OCH_3	D-11	2.63	E-11	2.53	F-11	3.32
3- OCH_3	D-12	2.60	E-12	2.54	F-12	3.28
4- OCH_3	D-13	2.62	E-13	2.57	F-13	3.30

Table 3. Inhibitory activity against EcGUS of target compounds **A** to **C** at 100 μM .

R						
	Compd.	Inhibitory rate (%)	Compd.	Inhibitory rate (%)	Compd.	Inhibitory rate (%)
2-F	A-1	48.8 \pm 2.8	B-1	46.9 \pm 5.5	C-1	19.1 \pm 1.2
3-F	A-2	49.2 \pm 1.3	B-2	47.3 \pm 5.2	C-2	47.1 \pm 6.9
4-F	A-3	41.1 \pm 8.3	B-3	44.3 \pm 3.9	C-3	48.0 \pm 3.6
2-Cl	A-4	38.0 \pm 4.8	B-4	40.3 \pm 4.3	C-4	32.6 \pm 3.2
3-Cl	A-5	36.7 \pm 6.9	B-5	31.1 \pm 4.3	C-5	44.0 \pm 2.7
4-Cl	A-6	36.1 \pm 3.7	B-6	36.9 \pm 3.3	C-6	47.0 \pm 4.8
2- CF_3	A-7	27.3 \pm 1.8	B-7	32.1 \pm 3.0	C-7	52.9 \pm 2.8
3- CF_3	A-8	25.3 \pm 0.8	B-8	28.2 \pm 1.6	C-8	47.2 \pm 1.5
4- CF_3	A-9	26.4 \pm 1.3	B-9	25.4 \pm 1.6	C-9	58.2 \pm 2.2
3,5- <i>di</i> - CF_3	A-10	26.8 \pm 3.1	B-10	30.2 \pm 3.5	C-10	41.7 \pm 1.9
4- OCH_3	A-11	28.7 \pm 5.2	B-11	17.7 \pm 1.5	C-11	45.9 \pm 2.7
—	DSL	76.2 \pm 3.0	—	—	—	—

(benzoxazole, R=2-CF₃, IR_{100 μM} = 32.1%), **B-8** (benzoxazole, R=3-CF₃, IR_{100 μM} = 28.2%), **B-9** (benzoxazole, R=4-CF₃, IR_{100 μM} = 25.4%), and **B-10** (benzoxazole, R=3,5-di-CF₃, IR_{100 μM} = 30.2%), respectively.

It also can be summarised that substituent groups on the benzene ring have a significant impact on enzymatic activities. Among benzimidazole or benzoxazole derivatives, fluorine (**A-1** to **3** and **B-1** to **3**) demonstrated better inhibitory effects over chloro (**A-4** to **6** and **B-4** to **6**), trifluoromethyl (**A-7** to **10** and **B-7** to **10**), or methoxyl (**A-11** and **B-11**) groups, with minimal variations based on substitution positions. In contrast, for benzothiazole derivatives, trifluoromethyl (**C-7** to **10**) exhibited potent inhibitory activity, especially when positioned *para* to the substituent. Specifically, **C-9** (R=4-CF₃) effectively enhanced the inhibitory rate to 58.2%, which showed more potent inhibition against EcGUS.

Upon further investigation on thiourea derivatives (Table 4), we found that urea compounds (**A-1** to **11**) generally outperformed thiourea compounds for 2-substituted benzimidazole derivatives (**D-1** to **13**). The position of the substituent on benzimidazole significantly influenced activity, with 6-substituted benzimidazole derivatives such as **E-6** (R=4-Cl, IR_{100 μM} = 57.8%), **E-9** (R=4-CF₃, IR_{100 μM} = 94.3%), and **E-13** (R=4-OCH₃, IR_{100 μM} = 63.8%) demonstrating better activities compared to 2-substituted compounds, particularly with *para*-substitution. Analogs belong to the

benzimidazole skeleton, trifluoromethyl proved to be a crucial moiety in 6-substituted benzimidazole derivatives (**E-9** displayed an inhibitory rate of 94.3%), while chloro exhibited positive effects in 8-substituted quinoline derivatives, including **F-4** (R=2-Cl, IR_{100 μM} = 50.9%) and **F-6** (R=4-Cl, IR_{100 μM} = 53.9%).

Inhibitory kinetic study of E-9 against EcGUS

The promising inhibitory effect of **E-9** on EcGUS *in vitro* motivated us to investigate its functional mechanism. To explore substrate-enzyme-inhibitor interaction, we conducted an analysis of its inhibitory kinetics using Lineweaver-Burk plot analysis⁴⁶. Enzyme activities were measured at different concentrations of AMX, DSL and **E-9** using substrate PNPG. Subsequently, their inhibitory behaviour was determined according to the intercept location of the regression line on Lineweaver-Burk plot^{47,48}. As depicted in Figure 4(A,C), the slopes remain unchanged by the presence of AMX or **E-9** while intercepts changed, which indicated that both AMX and **E-9** acted as uncompetitive inhibitors against EcGUS⁴⁹. As determined from the intersection point in the second quadrant, DSL was identified as a mixed inhibitor against EcGUS (Figure 4B). The results suggest that **E-9**, similar to AMX, exclusively binds to the enzyme-substrate complex (EcGUS-PNPG), and its binding site on EcGUS is likely consistent with that of AMX.

Molecular docking

To investigate the binding characteristics of **E-9** with the EcGUS receptor (PDB code: 3LPF) and analyse the structure-activity relationship of the target compounds, a molecular docking analysis was conducted utilising the MOE software platform^{50,51}. The representative characteristics for the binding of ligands (DSL, AMX, and synthetic compounds **E-9**, **E-4**, **A-9**, **D-9**, and **F-9**) with the EcGUS receptor were selected based on the binding energy and conformation with the most favourable interaction. The binding energy of **E-9** was determined to be -6.93 kJ·mol⁻¹, which was lower than that of DSL (-6.08 kJ·mol⁻¹), AMX (-6.55 kJ·mol⁻¹), and some synthetic compounds (**E-4**: -6.39 kJ·mol⁻¹, **A-9**: -6.51 kJ·mol⁻¹, **D-9**: -6.52 kJ·mol⁻¹, and **F-9**: -6.74 kJ·mol⁻¹), indicating that **E-9** exhibited a significantly stronger affinity for the EcGUS receptor. Specifically, **E-9** is strategically oriented within distinct active pockets: the benzimidazole moiety in **E-9** is positioned in a pocket through π-H bonding,

Table 4. Inhibitory activity against EcGUS of target compounds **D** to **F** at 100 μM.

R	Compd.	Inhibitory rate (%)	Compd.	Inhibitory rate (%)	Compd.	Inhibitory rate (%)
2-F	D-1	30.3±0.8	E-1	35.6±1.6	F-1	37.3±3.8
3-F	D-2	26.6±3.7	E-2	44.4±4.3	F-2	36.3±2.8
4-F	D-3	21.5±2.0	E-3	40.1±2.2	F-3	43.9±3.2
2-Cl	D-4	19.0±7.3	E-4	44.2±6.9	F-4	50.9±5.1
3-Cl	D-5	33.7±1.9	E-5	44.7±2.1	F-5	45.5±9.0
4-Cl	D-6	31.5±3.1	E-6	57.8±2.3	F-6	53.9±2.5
2-CF ₃	D-7	21.7±8.0	E-7	40.0±5.6	F-7	43.0±3.0
3-CF ₃	D-8	18.0±7.1	E-8	33.7±7.6	F-8	40.1±6.3
4-CF ₃	D-9	13.2±7.5	E-9	94.3±1.5	F-9	42.9±5.5
3,5-di-CF ₃	D-10	18.2±5.7	E-10	30.8±6.0	F-10	40.1±5.4
2-OCH ₃	D-11	19.3±1.7	E-11	37.0±2.8	F-11	42.5±3.8
3-OCH ₃	D-12	20.9±0.3	E-12	30.9±1.4	F-12	37.0±0.6
4-OCH ₃	D-13	37.5±3.4	E-13	63.8±1.6	F-13	52.6±1.7
—	DSL	76.2±3.0	—	—	—	—

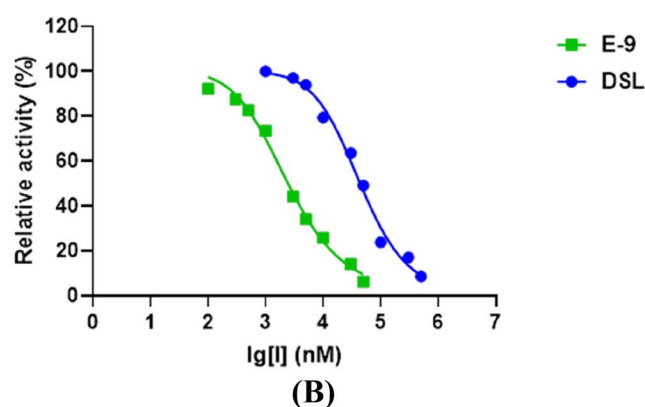
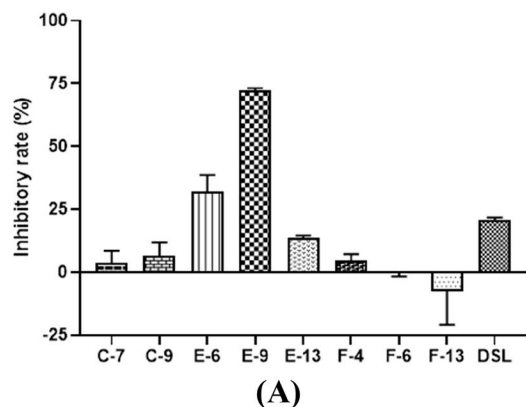


Figure 3. (A) Effects of partial target compounds on EcGUS at 10 μM (all data were expressed as mean±SD of triplicate reactions); (B) The dose-dependent inhibition curves of inhibitors (**E-9** and DSL) on PNPG-hydrolyzing activity of EcGUS.

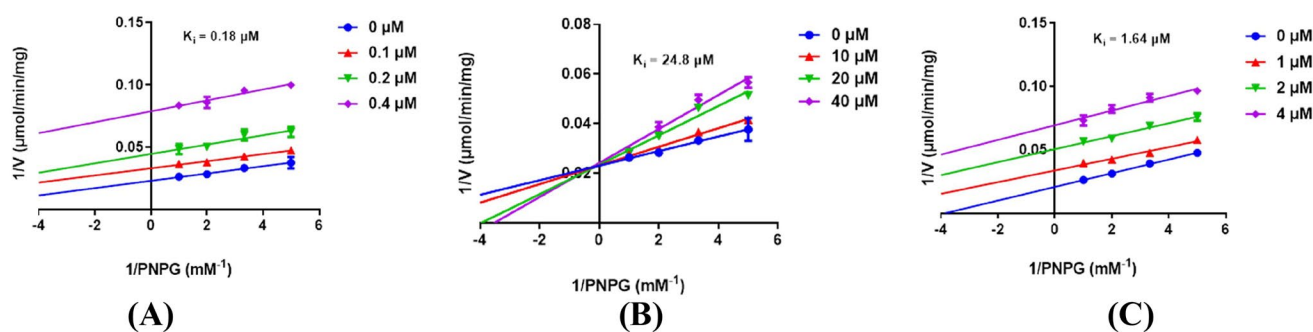


Figure 4. Lineweaver-Burk plots of AMX (A), DSL (B), and **E-9** (C) against EcGUS (all data were expressed as mean \pm SD of triplicate reactions).

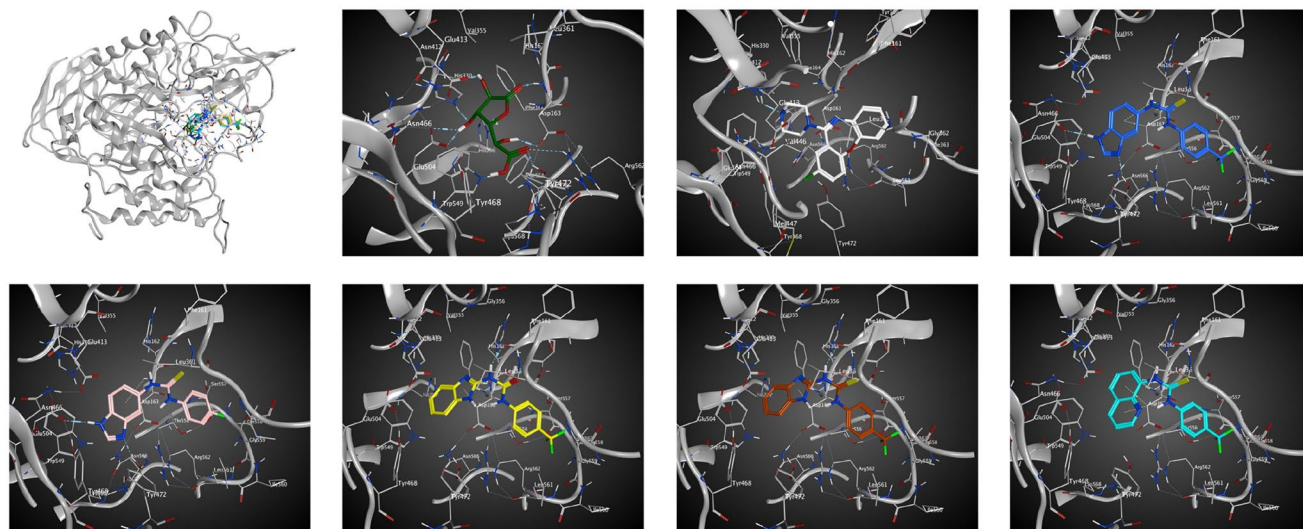


Figure 5. Ligand interactions of DSL (green), AMX (white), and synthetic compounds (**E-9**: blue, **E-4**: pink, **A-9**: yellow, **D-9**: brown, and **F-9**: cyan) with EcGUS (PDB code: 3LPF). The hydrogen bonds are shown as blue dashed lines. The interactions are shown as aqua dashed lines.

while the benzene ring and thiourea fragment closely accommodated in another pocket, thereby enhancing the stability of the **E-9**-EcGUS complex (Figure 5). Furthermore, the interaction between two nitrogen atoms in the benzimidazole moiety interact and the amino acids Tyr 472 and Glu 504 further strengthens the binding of **E-9** to the EcGUS receptor. However, it can be observed that the introduction of urea in **A-9**, fluorine in **E-4**, and the introduction of benzene-fused heterocycles in **D-9** and **F-9** each affect their interactions with the receptor EcGUS, potentially reducing their binding affinity compared to **E-9**, which may explain why their activities are not as potent as that of **E-9** (Tables 3 and 4). As a result, the docking models have highlighted the essential role of each molecular segment in the potent activity of **E-9**, laying the foundation for the future development of EcGUS inhibitors with improved activity.

Conclusion

In summary, a total of 72 (thio)urea derivatives were synthesised and subjected to biological assays in the search of novel EcGUS inhibitors. All target compounds displayed varying degrees of activity profiles in the EcGUS inhibition assay, with inhibition rates ranging from 13.2% to 94.3% at a concentration of 100 μ M. Notably, **E-9** exhibited a promising inhibitory effect ($IC_{50} = 2.68 \mu$ M) on EcGUS, exceeding the potency of a previously reported EcGUS

inhibitor, DSL ($IC_{50} = 45.8 \mu$ M). In addition, SAR analysis revealed that the incorporation of 6-substituted benzimidazole moieties may have a substantial impact on biological activity, suggesting the need for further detailed investigation. SAR analysis also indicated the crucial role of electron-withdrawing groups, particularly the trifluoromethyl group at the *para*-position of the phenyl ring, in enhancing the inhibitory activity of (thio)urea derivatives targets EcGUS. This specific substitution proved to be the most effective in enhancing inhibitory activity among all evaluated substituent groups. Furthermore, Lineweaver-Burk plot analysis indicated that **E-9** ($K_i = 1.64 \mu$ M) functioned as an uncompetitive inhibitor against EcGUS, sharing a similar mode of action with the EcGUS inhibitor AMX but differing from DSL. Molecular docking analysis revealed a binding energy of $-6.93 \text{ kJ}\cdot\text{mol}^{-1}$ for **E-9**, which was lower than that of DSL, AMX, and some synthetic compounds, suggesting a stronger affinity of **E-9** for the EcGUS receptor. Overall, these results suggest that **E-9** may serve as a potent EcGUS inhibitor, providing valuable insights and guidelines for the development of future EcGUS inhibitors.

Author contributions

Keren Xu: design, analysis and interpretation of the data; the drafting of the paper, revising; the final approval of the version to be published. Leyi Ying: analysis and interpretation of the data; the

drafting of the paper, revising. Titi Ying: analysis and interpretation of the data. Qihao Wu: conception; the drafting of the paper, revising. Lin Du: analysis and interpretation of the data; revising. Yanlei Yu: analysis and interpretation of the data. Youmin Ying: conception; revising. Bin Wei: conception, design; revising. Hong Wang - conception, design; the drafting of the paper, revising; the final approval of the version to be published. Zhikun Yang: conception, design, analysis and interpretation of the data; the drafting of the paper, revising; the final approval of the version to be published. All authors agree to be accountable for all aspects of the work.

Disclosure statement

The authors declare no known competing financial interests or personal relationships that could have appeared to influence the work reported in this paper.

Ethical approval statement

This research did not include any human subjects and animal experiments.

Funding

This work was financially supported by the programs of the National Key Research and Development Program of China (No. 2023YFA1506403, No. 2022YFC2804104), the National Natural Science Foundation of China (No. 42276137), the Key Research and Development Program of Zhejiang Province (No. 2021C03084), and the Natural Science Foundation of Zhejiang Province (No. LQ24H300012). We also gratefully acknowledge platform support from Zhejiang International Sci-Tech Cooperation Base for the Exploitation and Utilisation of Nature Product.

Data availability statement

Supplementary data to this article which consist of spectroscopy spectra of synthesised compounds can be found online.

References

- Kröner PT, Mody K, Farraye FA. Immune checkpoint inhibitor-related luminal GI adverse events. *Gastrointest Endosc.* 2019;90(6):881–892.
- Inagaki Y, Azuma K, Nakamura Y, Kouno S, Matsuda Y, Atagi S. Meaningful symptoms of immune checkpoint inhibitor therapy-related gastrointestinal adverse events in patients with inflammatory bowel disease. *J Clin Oncol.* 2020;38(15):1748–1749.
- Wu W, Li WX, Huang CH. Phospholipase A₂, a nonnegligible enzyme superfamily in gastrointestinal diseases. *Biochimie.* 2022;194:79–95.
- Wallace BD, Wang HW, Lane KT, Scott JE, Orans J, Koo JS, Venkatesh M, Jobin C, Yeh LA, Mani S, et al. Alleviating cancer drug toxicity by inhibiting a bacterial enzyme. *Science.* 2010;330(6005):831–835.
- Wallace BD, Redinbo MR. The human microbiome is a source of therapeutic drug targets. *Curr Opin Chem Biol.* 2013;17(3):379–384.
- McIntosh FM, Maison N, Holtrop G, Young P, Stevens VJ, Ince J, Johnstone AM, Lobleby GE, Flint HJ, Louis P. Phylogenetic distribution of genes encoding β -glucuronidase activity in human colonic bacteria and the impact of diet on faecal glycosidase activities. *Environ Microbiol.* 2012;14(8):1876–1887.
- Patel AG, Kaufmann SH. Targeting bacteria to improve cancer therapy. *Science.* 2010;330(6005):766–767.
- Abet V, Filace F, Recio J, Builla JA, Burgos C. Prodrug approach: an overview of recent cases. *Eur J Med Chem.* 2017;127:810–827.
- Pommier Y. Topoisomerase I inhibitors: camptothecins and beyond. *Nat Rev Cancer.* 2006;6(10):789–802.
- LoGuidice A, Wallace BD, Bendel L, Redinbo MR, Boelsterli UA. Pharmacologic targeting of bacterial β -glucuronidase alleviates nonsteroidal anti-inflammatory drug-induced enteropathy in mice. *J Pharmacol Exp Ther.* 2012;341(2):447–454.
- Fortun PJ, Hawkey CJ. Nonsteroidal anti-inflammatory drugs and the small intestine. *Curr Opin Gastroenterol.* 2005;21(2):169–175.
- Maiden L. Capsule endoscopic diagnosis of nonsteroidal anti-inflammatory drug-induced enteropathy. *J Gastroenterol.* 2009;44 Suppl 19(S19):64–71.
- Ahmad S, Hughes MA, Yeh LA, Scott JE. Potential repurposing of known drugs as potent bacterial β -glucuronidase inhibitors. *J Biomol Screen.* 2012;17(7):957–965.
- Fittkau M, Voigt W, Holzhausen HJ, Schmoll HJ. Saccharic acid 1,4-lactone protects against CPT-11-induced mucosa damage in rats. *J Cancer Res Clin Oncol.* 2004;130(7):388–394.
- Levy GA. The preparation and properties of β -glucuronidase. IV. Inhibition by sugar acids and their lactones. *Biochem J.* 1952;52(3):464–472.
- Wallace BD, Roberts AB, Pollet RM, Ingle JD, Biernat KA, Pellock SJ, Venkatesh MK, Guthrie L, O'Neal SK, Robinson SJ, et al. Structure and inhibition of microbiome β -glucuronidases essential to the alleviation of cancer drug toxicity. *Chem Biol.* 2015;22(9):1238–1249.
- Awolade P, Cele N, Kerru N, Gummidi L, Oluwakemi E, Singh P. Therapeutic significance of β -glucuronidase activity and its inhibitors: a review. *Eur J Med Chem.* 2020;187:111921.
- Wei B, Yang W, Yan ZX, Zhang QW, Yan R. Prenylflavonoids sanggenon C and kuwanon G from mulberry (*Morus alba* L.) as potent broad-spectrum bacterial β -glucuronidase inhibitors: biological evaluation and molecular docking studies. *J Funct Food.* 2018;48:210–219.
- Sun CP, Yan JK, Yi J, Zhang XY, Yu ZL, Huo XK, Liang JH, Ning J, Feng L, Wang C, et al. The study of inhibitory effect of natural flavonoids toward β -glucuronidase and interaction of flavonoids with β -glucuronidase. *Int J Biol Macromol.* 2020;143:349–358.
- Li XN, Hua LX, Zhou TS, Wang KB, Wu YY, Emam M, Bao XZ, Chen J, Wei B. Cinnamic acid derivatives: inhibitory activity against *Escherichia coli* β -glucuronidase and structure-activity relationships. *J Enzyme Inhib Med Chem.* 2020;35(1):1372–1378.
- Yu HF, Cheng YC, Wu CM, Ran K, Wei B, Xu YK, Shan WG, Ying YM, Zhan ZJ. Diverse diterpenoids with α -glucosidase and β -glucuronidase inhibitory activities from *Euphorbia milii*. *Phytochemistry.* 2022;196:113106.
- Rao GW, Yu HF, Zhang ML, Cheng YC, Ran K, Wang JW, Wei B, Li M, Shan WG, Zhan ZJ, et al. α -Glucosidase and bacterial β -glucuronidase Inhibitors from the stems of *Schisandra sphaerandra* Staph. *Pharmaceuticals.* 2022;15(3):329.
- Wang PP, Wu RR, Jia YF, Tang PP, Wei B, Zhang QW, Wang VYF, Yan R. Inhibition and structure-activity relationship of dietary flavones against three Loop 1-type human gut microbial β -glucuronidases. *Int J Biol Macromol.* 2022;220:1532–1544.

24. Xia LJ, Wan L, Gao A, Yu YX, Zhou SY, He Q, Li G, Ren H, Lian XL, Zhao DH, et al. Targeted inhibition of gut bacterial β -glucuronidases by octyl gallate alleviates mycophenolate mofetil-induced gastrointestinal toxicity. *Int J Biol Macromol*. 2024;264(Pt 1):130145.
25. Chen L, Hou XD, Zhu GH, Huang J, Guo ZB, Zhang YN, Sun JM, Ma LJ, Zhang SD, Hou J, et al. Discovery of a botanical compound as a broad-spectrum inhibitor against gut microbial β -glucuronidases from the Tibetan medicine *Rhodiola crenulate*. *Int J Biol Macromol*. 2024;267(Pt 1):131150.
26. Zhou TS, Wei B, He M, Li YS, Wang YK, Wang SJ, Chen JW, Zhang HW, Cui ZN, Wang H. Thiazolidin-2-cyanamides derivatives as novel potent *Escherichia coli* β -glucuronidase inhibitors and their structure-inhibitory activity relationships. *J Enzyme Inhib Med Chem*. 2020;35(1):1736–1742.
27. Li YS, He M, Zhou TS, Wang Q, He LL, Wang SJ, Hu B, Wei B, Wang H, Cui ZN. 2,5-Disubstituted furan derivatives containing 1,3,4-thiadiazole moiety as potent α -glucosidase and *E. coli* β -glucuronidase inhibitors. *Eur J Med Chem*. 2021;216:113322.
28. Zhou TS, He LL, He J, Yang ZK, Zhou ZY, Du AQ, Yu JB, Li YS, Wang SJ, Wei B, et al. Discovery of a series of 5-phenyl-2-furan derivatives containing 1,3-thiazole moiety as potent *Escherichia coli* β -glucuronidase inhibitors. *Bioorg Chem*. 2021;116:105306.
29. Saitta KS, Zhang C, Lee KK, Fujimoto K, Redinbo MR, Boelsterli UA. Bacterial β -glucuronidase inhibition protects mice against enteropathy induced by indomethacin, ketoprofen or diclofenac: mode of action and pharmacokinetics. *Xenobiotica*. 2014;44(1):28–35.
30. Perveen S, Mustafa S, Qamar K, Dar A, Khan KM, Choudhary MI, Khan A, Voelter W. Anti-proliferative effects of novel urea derivatives against human prostate and lung cancer cells and their inhibition of β -glucuronidase activity. *Med Chem Res*. 2014;23(3):1099–1113.
31. Taha M, Ismail NH, Jamil W, Khan KM, Salar U, Kashif SM, Rahim F, Latif Y. Synthesis and evaluation of unsymmetrical heterocyclic thioureas as potent β -glucuronidase inhibitors. *Med Chem Res*. 2015;24(8):3166–3173.
32. Khan KM, Khan M, Ambreen N, Rahim F, Naureen S, Perveen S, Choudhary MI, Voelter W. Synthesis and β -glucuronidase inhibitory potential of benzimidazole derivatives. *Med Chem*. 2012;8(3):421–427.
33. Taha M, Ismail NH, Imran S, Selvaraj M, Rashwan H, Farhanah FU, Rahim F, Kesavanarayanan KS, Ali M. Synthesis of benzimidazole derivatives as potent β -glucuronidase inhibitors. *Bioorg Chem*. 2015;61:36–44.
34. Kamil A, Akhtar S, Noureen S, Saify ZS, Jahan S, Khan KM, Rahim F, Taha M, Mushtaq N, Arif M, et al. 2-(2'-Pyridyl)benzimidazole analogs and their β -glucuronidase inhibitory activity. *J Chem Soc Pak*. 2015;37(4):787–791.
35. Zawawi NKNA, Taha M, Ahmat N, Wadood A, Ismail NH, Rahim F, Ali M, Abdullah N, Khan KM. Novel 2,5-disubstituted-1,3,4-oxadiazoles with benzimidazole backbone: a new class of β -glucuronidase inhibitors and in silico studies. *Bioorg Med Chem*. 2015;23(13):3119–3125.
36. Khan KM, Rahim F, Halim SA, Taha M, Khan M, Perveen S, Haq Z, Mesaik MA, Choudhary MI. Synthesis of novel inhibitors of β -glucuronidase based on benzothiazole skeleton and study of their binding affinity by molecular docking. *Bioorg Med Chem*. 2011;19(14):4286–4294.
37. Taha M, Ismail NH, Imran S, Selvaraj M, Rahim F. Synthesis of novel inhibitors of β -glucuronidase based on the benzothiazole skeleton and their molecular docking studies. *RSC Adv*. 2016;6(4):3003–3012.
38. Taha M, Arbin M, Ahmat N, Imran S, Rahim F. Synthesis: small library of hybrid scaffolds of benzothiazole having hydrazone and evaluation of their β -glucuronidase activity. *Bioorg Chem*. 2018;77:47–55.
39. Taha M, Sultan S, Nuzar HA, Rahim F, Imran S, Ismail NH, Naz H, Ullah H. Synthesis and biological evaluation of novel N-arylidenequinoline-3-carbohydrazides as potent β -glucuronidase inhibitors. *Bioorg Med Chem*. 2016;24(16):3696–3704.
40. Chen YL, Zhao YL, Lu CM, Tzeng CC, Wang JP. Synthesis, cytotoxicity, and anti-inflammatory evaluation of 2-(furan-2-yl)-4-(phenoxy)quinoline derivatives. Part 4. *Bioorg Med Chem*. 2006;14(13):4373–4378.
41. Cheng KW, Tseng CH, Yang CN, Tzeng CC, Cheng TC, Leu YL, Chuang YC, Wang JY, Lu YC, Chen YL, et al. Specific inhibition of bacterial β -glucuronidase by pyrazolo[4,3-c]quinoline derivatives via a pH-dependent manner to suppress chemotherapy-induced intestinal toxicity. *J Med Chem*. 2017;60(22):9222–9238.
42. Cheng KW, Tseng CH, Tzeng CC, Leu YL, Cheng TC, Wang JY, Chang JM, Lu YC, Cheng CM, Chen JJ, et al. Pharmacological inhibition of bacterial β -glucuronidase prevents irinotecan-induced diarrhea without impairing its antitumor efficacy *in vivo*. *Pharmacol Res*. 2019;139:41–49.
43. Taha M, Uddin N, Ali M, Anouar EH, Rahim F, Khan G, Farooq RK, Gollapalli M, Iqbal N, Farooq M, et al. Inhibition potential of phenyl linked benzimidazole-triazolothiadiazole modular hybrids against β -glucuronidase and their interactions thereof. *Int J Biol Macromol*. 2020;161:355–363.
44. Daina A, Michielin O, Zoete V. SwissADME: a free web tool to evaluate pharmacokinetics, drug-likeness and medicinal chemistry friendliness of small molecules. *Sci Rep*. 2017;7(1):42717.
45. Walters WP. Going further than Lipinski's rule in drug design. *Expert Opin Drug Discov*. 2012;7(2):99–107.
46. Yamamoto K, Miyake H, Kusunoki M, Osaki S. Crystal structures of isomaltase from *Saccharomyces cerevisiae* and in complex with its competitive inhibitor maltose. *Febs J*. 2010;277(20):4205–4214.
47. Xin H, Qi XY, Wu JJ, Wang XX, Li Y, Hong JY, He W, Xu W, Ge GB, Yang L. Assessment of the inhibition potential of Licochalcone A against human UDP-glucuronosyltransferases. *Food Chem Toxicol*. 2016;90:112–122.
48. Lv X, Wang XX, Hou J, Fang ZZ, Wu JJ, Cao YF, Liu SW, Ge GB, Yang L. Comparison of the inhibitory effects of tolcapone and entacapone against human UDP-glucuronosyltransferases. *Toxicol Appl Pharmacol*. 2016;301:42–49.
49. Bowd AC. Why is uncompetitive inhibition so rare? A possible explanation, with implications for the design of drugs and pesticides. *FEBS Lett*. 1986;203(1):3–6.
50. Yang ZK, Cai Y, Yang X, Li YS, Wu QH, Yu YL, Chen Z, Wei B, Tian JM, Bao XZ, et al. Novel benzo five-membered heterocycle derivatives as P-glycoprotein inhibitors: design, synthesis, molecular docking, and anti-multidrug resistance activity. *J Med Chem*. 2023;66(8):5550–5566.
51. Yang ZK, Yang X, Li YS, Cai Y, Yu YL, Zhuang WY, Sun XR, Li QY, Bao XZ, Ye XY, et al. Design, synthesis and biological evaluation of novel phenylfuran-bisamide derivatives as P-glycoprotein inhibitors against multidrug resistance in MCF-7/ADR cell. *Eur J Med Chem*. 2023;248:115092.